

THE EFFECT OF VARIABLE MAGNETIC FIELD ON HEAT TRANSFER AND FLOW ANALYSIS OF UNSTEADY SQUEEZING NANOFLUID FLOW BETWEEN PARALLEL PLATES USING GALERKIN METHOD

by

**Mohammad RAHIMI-GORJI^{a,*}, Oveis POURMEHRAN^a,
Mofid GORJI-BANDPY^b, and Davood Domiri GANJI^b**

^aYoung Researchers and Elite Club, Gorgan Branch, Islamic Azad University, Gorgan, Iran

^bMechanical Engineering Department, Babol Noshirvani University of Technology, Babol, Iran

Original scientific paper

<https://doi.org/10.2298/TSCI160524180R>

This paper presents a thermal and flow analysis of an unsteady squeezing nanofluid flow and heat transfer using nanofluid based on Brinkman model in presence of variable magnetic field. Galerkin method is used to solve the non-linear differential equations governing the problem. Squeezing flow between parallel plates is very applicable in the many industries and it means that one or both of the parallel plates have vacillation. The effects of active parameters such as the Hartman number, squeeze number, and heat source parameter are discussed. Results for temperature distribution and velocity profile, Nusselt number, and skin friction coefficient by Galerkin method are presented. As can be seen in results, the values of Nusselt number and skin friction coefficient for CuO is better than Al₂O₃. Also, according to figures, as nanofluid volume fraction increases, Nusselt number increases and skin friction coefficient decreases, increase in the Hartman number results in an increase in velocity and temperature profiles and an increase in squeeze number can be associated with the decrease in the velocity.

Key words: flow analysis, squeezing nanofluid flow, heat transfer, Galerkin method

Introduction

Nanofluids are fluids consist of nanoparticles (nanometer-sized particles of metals, oxides, carbides, nitrides, or nanotubes). Nanofluids demonstrate increased thermal properties, amongst them: higher thermal conductivity and heat transfer coefficients compared to the base fluid. The nanofluid can be applied to engineering problems, such as cooling of electronic equipment, heat exchangers, and chemical processes. Nanofluid contains a base fluid usually water, ethylene glycol, oil or engine oil and nanopowders such as Cu, CuO, Al₂O₃, TiO₂ or nanodiamond and usually a dispersant or surfactant to keep the nanoparticles suspension stable. The main features of using nanofluids are increasing the heat transfer and viscosity improvement. Nanoparticles that are immersed in the base fluid will transfer heat with their Brownian motion and interactions. This advanced technique, which utilizes a mixture of nanoparticles and the base fluid, was first suggested by [1] in order to develop heat transfer fluids with considerably

*Corresponding author, e-mail: m69.rahimi@yahoo.com

**Now in Young Researches and Elite Club, Behshahr Branch, Islamic Azad University, Behshahr, Mazandaran, Iran

higher conductivities. An admirable collection of the published papers on nanofluids can be found in the book by Das *et al.* [2].

Lately, the concept of a nanofluid has been proposed as a route for increasing the performance of the heat transfer rates in the liquids that are currently applied. Materials with sizes of nanometers have unique physical and chemical properties [2]. It has been understood that the presence of nanoparticles within the fluid can extremely increase the effective thermal conductivity of the fluid and, as a consequence, increase the heat transfer characteristics. An excellent collection of works on this topic can be found in the book by Das *et al.* [2] and in the review papers by [3-5]. Rahimi-Gorji *et al.* [6] studied the optimization of micro-channel heat sink geometry cooled by different nanofluids using response-surface method (RSM) analysis. Several studies have been performed on prediction of thermal conductivity of nanofluids [7-10].

A numerical investigation on the heat transfer increasing due to adding nanoparticles in a differentially heated compound is reported by [11]. Hatami and Ganji [12] applied a numerical method to find the most accurate solution for the natural convection of the sodium alginate non-Newtonian nanofluid flow between two vertical plates. As a main result from their work, it is observed that by increasing the Prandtl number, velocity profiles and temperature values increased significantly, also Cu as nanoparticles had larger velocity and temperature values than Ag. Pourmehran *et al.* [13] examined the optimization of micro-channel heat sink performance cooled by KKL based in saturated porous medium.

Khan and Pop [14] carried out research on boundary-layer flow of a nanofluid past a stretching sheet. Their model used for the nanofluid incorporates the effects of Brownian motion and thermophoresis. The heat transfer characteristics in the squeezed flow over a porous surface analyzed by [15]. Domairy and Aziz [16] investigated MHD squeezing flow of a viscous fluid between parallel disks.

In recent years, much attention has been dedicated to the newly developed methods to construct an analytic solution of equation such as Collocation method (CM), Least Square method (LSM), and Galerkin method (GM) which are introduced by Ozisik [17] for using in the heat transfer problems. Many of equations in the heat transfer problems can be solved by these analytical methods that called the weighted residuals methods (WRM). Rahimi-Gorji *et al.* [18] performed an analytical analysis of particle motion in the non-Newtonian fluid using CM. Pourmehran *et al.* [19] analytically investigated the heat transfer of nanofluid flow between two parallel plates in order to show the influence of different nanoparticles on heat transfer by LSM, CM, and numerical method. Hendi and Albugami [20] solved Fredholm-Volterra integral equation using CM and GM. Legendre wavelet GM has been used for solving ODE with non-analytic solution by [21]. Hatami *et al.* [22] has investigated heat transfer and flow analysis for a non-Newtonian third grade nanofluid flow in porous medium of a hollow vessel in presence of magnetic field by using LSM, GM, and numerical method.

In this paper, the viscosity of nanofluid and effective thermal conductivity are calculated by Brinkman correlation [23]. Also in the present paper, GM is used to solve non-linear differential equations governing the problem of unsteady squeezing nanofluid flow and heat transfer using nanofluid based on Brinkman model in presence of variable magnetic field. Nusselt number and skin friction coefficient are presented. The effects of active parameters such as the Hartman number, squeeze number, and heat source parameter are discussed. Heat transferring performance of the parallel plates is investigated by using CuO-water and Al₂O₃-water nanofluids as coolant agent. Results for temperature distribution and velocity profile, Nusselt number, and skin friction coefficient by GM are presented.

Description of the problem

The problem to be studied is the 2-D heat transfer in the unsteady squeezing flow of an incompressible nanofluid between the infinite parallel plates as shown in fig. 1. The distance between the plates is $2l(1 - \alpha t)^{1/2}$. For $\alpha > 0$, the two plates are squeezed until they touch $t = 1/\alpha$ and for $\alpha < 0$ the two plates are separated. A time variable magnetic field $[\vec{B} = B\vec{e}, B = B_0(1 - \alpha t)]a$ is assumed to be applied towards direction y .

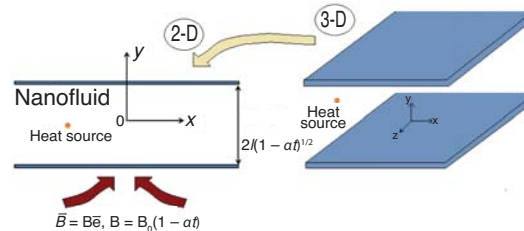


Figure 1. Schematic of the problem (nanofluid between parallel plates)

As can be seen in fig. 1, a heat source $Q = Q_0/(1 - \alpha t)$ is utilized between two plates. Also, the electromagnetic force and the electric current are defined by F and J , respectively. In this problem, the fluid is a water based nanofluid containing CuO nanoparticles. The nanofluid is a two component mixture with the following assumptions: incompressible, no-chemical reaction, and negligible radiative heat transfer. Nanosolid-particles, and the base fluid are in thermal equilibrium and no slip occurs between them. The thermophysical properties of the nanofluid are given in tab. 1 [24].

Table 1. Thermophysical properties of water and nanoparticles [24]

	ρ [kgm ⁻³]	C_p [Jkg ⁻¹ K ⁻¹]	k [Wm ⁻¹ K ⁻¹]	μ [Nsm ⁻²]	d_p [nm]
Pure water	997.1	4179	0.613	0.001003	—
CuO	6500	540	18	—	29
Al ₂ O ₃	3970	765	25	—	47

Take y to be perpendicular to the plates and assume u and v to be the velocity components in the x - and y - directions, respectively. The governing equations for momentum and energy in unsteady 2-D flow of a nanofluid are [25]:

$$u_x + v_y = 0 \quad (1)$$

$$\rho_{nf} (u_t + u u_x + v u_y) = -p_x + \mu_{nf} (u_{xx} + u_{yy}) - \sigma_{nf} B_0^2 u \quad (2)$$

$$\rho_{nf} (v_t + u v_x + v v_y) = -p_y + \mu_{nf} (v_{xx} + v_{yy}) \quad (3)$$

$$T_t + u T_x + v T_y = \frac{k_{nf}}{(\rho C_p)_{nf}} (T_{xx} + T_{yy}) + \frac{Q}{(\rho C_p)_{nf}} \quad (4)$$

where P is the pressure, ρ_{nf} – the effective density and $(\rho C_p)_{nf}$ – the effective heat capacity of the nanofluid, σ_{nf} – the effective electrical conductivity of nanofluid, and k_{nf} – the effective thermal conductivity of the nanofluid are defined [6]:

$$\rho_{nf} = (1 - \phi) \rho_f + \phi \rho_s \quad (5)$$

$$\mu_{nf} = \frac{\mu_f}{(1 - \phi)^{2.5}} \quad (6)$$

$$(\rho C_p)_{nf} = (1 - \phi)(\rho C_p)_f + (\rho C_p)_s \quad (7)$$

$$\frac{\sigma_{nf}}{\sigma_f} = 1 + \frac{3 \left(\frac{\sigma_s}{\sigma_f} - 1 \right) \phi}{\left(\frac{\sigma_s}{\sigma_f} + 2 \right) - \left(\frac{\sigma_s}{\sigma_f} - 1 \right) \phi} \quad (8)$$

$$\frac{k_{nf}}{k_f} = \frac{k_s + 2k_f - 2\phi(k_f - k_s)}{k_s + 2k_f + 2\phi(k_f - k_s)} \quad (9)$$

where $\mu_{nf} = \mu_f / (1 - \phi)^{2.5}$ is viscosity of the nanofluid, as given originally by Brinkman.

The relevant boundary conditions are:

$$\begin{aligned} v = v_w = \frac{dh}{dt}, \quad T = T_H \quad \text{at } y = h(t) \\ v = \frac{\partial u}{\partial y} = \frac{\partial T}{\partial y} = 0, \quad \text{at } y = 0 \end{aligned} \quad (10)$$

The following dimensionless groups are introduced:

$$\eta = \frac{y}{l(1 - \alpha t)^{0.5}}, \quad u = \frac{\alpha x}{2(1 - \alpha t)} f'(\eta), \quad v = -\frac{\alpha l}{2(1 - \alpha t)^{0.5}} f(\eta), \quad \theta = \frac{T}{T_H} \quad (11)$$

By using the dimensionless parameters and substituting eq. (14) into eqs. (2)-(4) and removing the pressure gradient from obtained equations, we get the following ODE:

$$f^{iv} - S \frac{A_1}{A_4} (\eta f''' + 3f'' + f' f'' - f f''') - \text{Ha}^2 \frac{A_5}{A_4} f'' = 0 \quad (12)$$

$$\theta'' + \text{Pr} S \frac{A_2}{A_3} (f \theta' - \eta \theta') + \frac{Hs}{A_3} \theta = 0 \quad (13)$$

where A_1, A_2, A_3, A_4 , and A_5 are dimensionless constants given by:

$$A_1 = \frac{\rho_{nf}}{\rho_f}, \quad A_2 = \frac{(\rho C_p)_{nf}}{(\rho C_p)_f}, \quad A_3 = \frac{k_{eff}}{k_f}, \quad A_4 = \frac{\mu_{eff}}{\mu_f}, \quad A_5 = \frac{\sigma_{nf}}{\sigma_f} \quad (14)$$

and the boundary conditions (10) become:

$$\begin{aligned} f(0) = 0, \quad f''(0) = 0 \\ f(1) = 1, \quad f'(1) = 0 \\ \theta'(0) = 0, \quad \theta(1) = 1 \end{aligned} \quad (15)$$

Here $\text{Ha} = l B_0 (\sigma_f / \mu_f)^{-1/2}$ is the Hartman number, $S = \alpha l^2 / 2 v_f$ – the squeeze number, $\text{Pr} = [\mu_f (\rho C_p)_f] / \rho_f k_f$ – Prandtl number, and $Hs = Q_0 l^2 / k_f$ – the heat source parameter.

Two significant characteristics that analyzed in this work are the Nusselt number and skin friction coefficient which are defined:

$$C_f^* = \frac{\mu_{nf} \left(\frac{\partial u}{\partial y} \right)_{y=h(t)}}{\rho_{nf} v_w^2}, \quad \text{Nu}^* = \frac{-l k_{nf} \left(\frac{\partial T}{\partial y} \right)_{y=h(t)}}{k_f T_H} \quad (16)$$

Using variables (14), we get

$$C_f = \left| \left(\frac{A_1}{A_4} \right) f''(1) \right|, \quad \text{Nu} = |A_3 \theta'(1)| \quad (17)$$

Applied analytical method

A significant point that should be considered is to provide some background knowledge about the mathematical methods utilized. Therefore, in this section, some basic relationships and theories concerning GM are presented.

Many advantages of WRM especially GM compared to other analytical make them more valuable and motivate researchers to use them for solving problems. Some of these advantages are listed below [6]:

- The WRM solve the equations directly and no simplifications are needed.
- They do not need any perturbation, linearization or small parameter versus homotopy perturbation method and parameter perturbation method.
- They are simple and powerful compared to numerical methods and achieve final results faster than numerical procedures while their results are acceptable and have excellent agreement with numerical outcomes, furthermore their accuracy can be increased by increasing the statements of the trial functions.
- They do not need to determine the auxiliary parameter and auxiliary function versus homotopy analysis method.

Galerkin method

Suppose a differential operator, D , is applied on a function u to produce a function, p .

$$D[u(x)] = p(x) \quad (18)$$

where u is approximated by a function \tilde{u} , which is a linear combination of basic functions chosen from a linearly in dependent set. That is:

$$u \cong \tilde{u} = \sum_{i=1}^n c_i \varphi_i \quad (19)$$

Now, when substituted into the differential operator, D , the result of the operations is not, in general, $p(x)$. Hence an error or residual will exist:

$$E(x) = R(x) = D[\tilde{u}(x)] - p(x) \neq 0 \quad (20)$$

The main idea of the GM is to force the residual to zero in some average sense over the domain. That is:

$$\int_x R(x) W_i(x) dx = 0, \quad i = 1, 2, \dots, n \quad (21)$$

where the number of weight functions, W_i , is exactly equal the number of unknown constants c_i in \tilde{u} function. The result is a set of n algebraic equations for the unknown constants c_i . In GM weight functions are [18]:

$$W_i = \frac{\partial \tilde{u}}{\partial g_i}, \quad i = 1, 2, \dots, n \quad (22)$$

Now GM is applied to the eqs. (12) and (13). First consider the trial function:

$$\begin{aligned} f(\eta) &= \eta^3 + c_1(\eta^3 - \eta) + c_2(\eta^3 - \eta^5) + c_3(\eta^3 - \eta^7) \\ \theta(\eta) &= 1 + c_4(1 - \eta^3) + c_5(1 - \eta^5) + c_6(1 - \eta^6) \end{aligned} \quad (23)$$

Which satisfies the initial condition in eqs. (12) and (13). Using eq. (22), weight functions will be obtained:

$$\begin{aligned} W_1 &= \eta^3 - \eta, & W_2 &= \eta^3 - \eta^5, & W_3 &= \eta^3 - \eta^7 \\ W_4 &= 1 - \eta^3, & W_5 &= 1 - \eta^5, & W_6 &= 1 - \eta^6 \end{aligned} \quad (24)$$

Applying eq. (21), a set of algebraic equations is defined and solving this set of equations, all constant coefficients will be calculated.

Finally $f(\eta)$ and $\theta(\eta)$ functions for CuO-water nanofluid when $d_p = 29$ nm and $\phi = 0.04$ will be calculated:

$$\begin{aligned} f(\eta) &= -0.35\eta^3 + 1.42\eta - 0.069\eta^5 - 0.0037\eta^7 \\ \theta(\eta) &= 0.76 + 0.44\eta^3 - 0.305\eta^5 + 0.19\eta^7 \end{aligned} \quad (25)$$

Results and discussion

In this study, after investigating of the heat transfer in the unsteady squeezing flow of an incompressible nanofluid between the infinite parallel plates. It is noteworthy that the viscosity of nanofluid and effective thermal conductivity are calculated by Brinkman correlation. The GM is used to solve this problem. Table 1 present properties of the nanoparticles and base fluid. The comparison between present work and Mustafa *et al.* work [25] is depicted in fig. 2 that shows an excellent agreement.

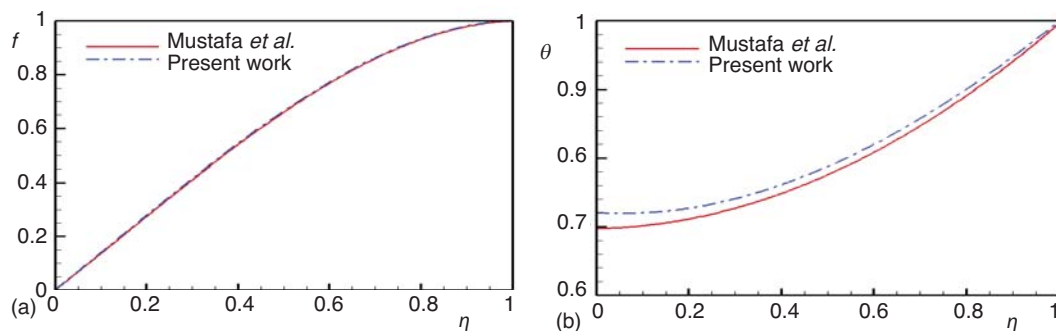


Figure 2. Comparison between present work and Mustafa *et al.* [25] (CuO-water nanofluid for (a) velocity profile, (b) temperate profile when; $\phi = 0.04$, $d_p = 29$ nm, $Ha = 1$, $S = 1$, and $Hs = -1$)

In fig. 3, two nanofluids (CuO-water and Al_2O_3 -water) are shown that their Nusselt number and skin friction coefficient are compared. As can be seen in this figure, the values of Nusselt number and skin friction coefficient for CuO-water is better than Al_2O_3 -water.

The construction of the all following figures, figs. 4-10, which show the effects of some important parameters on velocity profile, temperature distribution, Nusselt number, and skin friction coefficient, is based on CuO-water. Figure 4 demonstrates the effect of volume fraction (ϕ) of CuO-water nanofluid on Nusselt number and skin friction coefficient. According to this figure, as nanofluid volume fraction increases, Nusselt number increases and skin friction coefficient decreases.

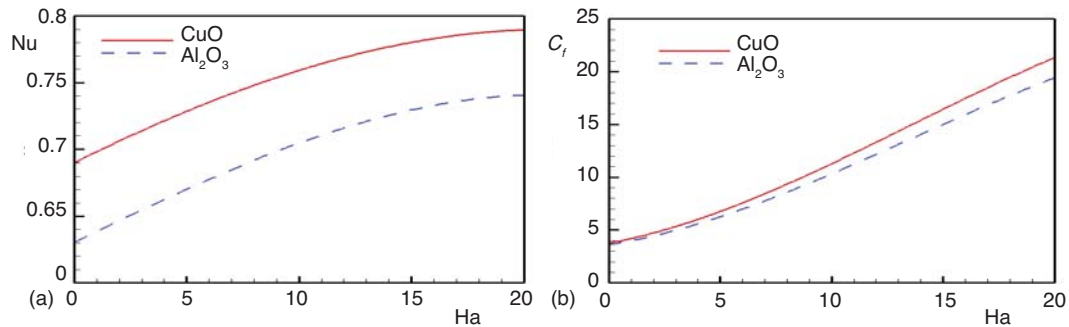


Figure 3. Comparison between CuO-water and Al₂O₃-water nanofluids (a) Nusselt number, (b) skin friction coefficient when; $\phi = 0.04$, $dp = 29$ nm, $Ha = 1$, $S = 1$, and $Hs = -1$

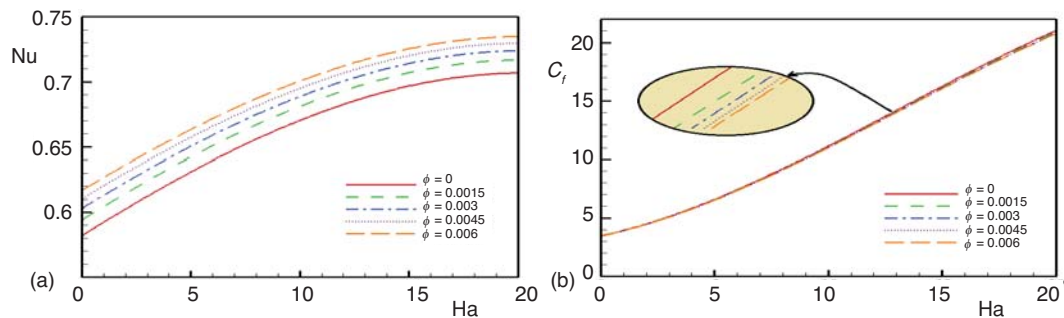


Figure 4. Effect of volume fraction of CuO-water nanofluid on (a) Nusselt number, (b) skin friction coefficient when; $Pr = 6.2$, $Hs = -1$, and $S = 1$

Also, contours of fig. 5 confirm these effects of volume fraction and Hartmann number on Nusselt number and skin friction coefficient. The effect of the Hartmann number on velocity and temperature profiles is shown in fig. 6. As seen in this figure, increase in the Hartmann number results in an increase in velocity and temperature profiles.

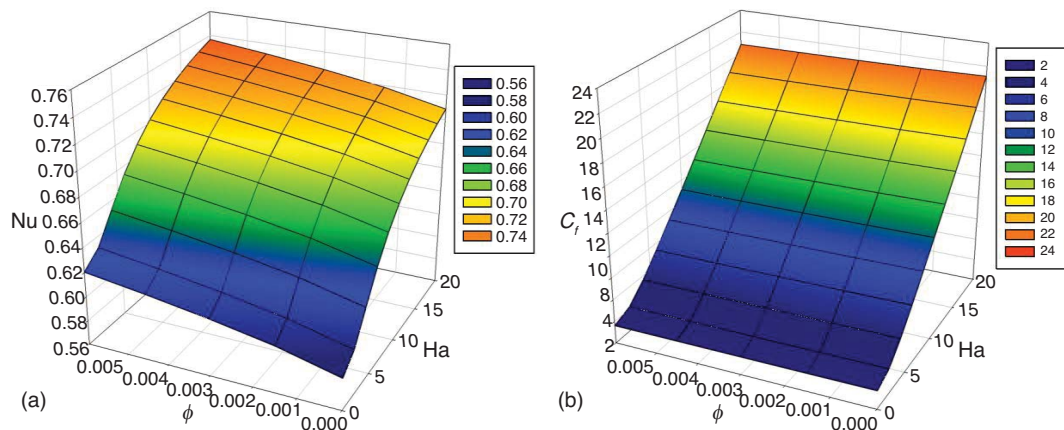


Figure 5. Contours for effects of volume fraction and Hartman number on (a) Nusselt number, (b) skin friction coefficient when; $S = 1$, $Hs = -1$, and $dp = 29$ nm (CuO-water) (for color image see journal web site)

Figure 7 illustrates the effect of the squeeze number on velocity and temperature profiles. It is quite obvious that when two plates move together, thermal boundary-layer thickness increases as the absolute magnitude of the squeeze number enhances. The temperature is relatively high when the plates are moving towards each other. Also, an increase in squeeze number can be associated with the decrease in the velocity.

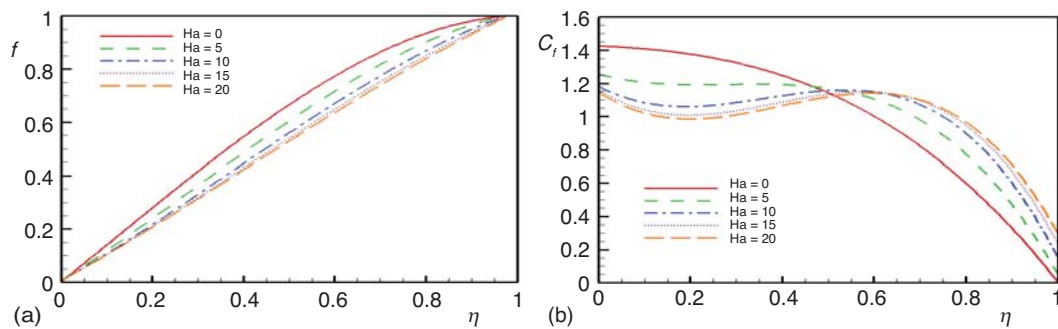


Figure 6. Effect of the Hartmann number on velocity and temperature profiles when; $Pr = 6.2$, $Hs = -1$, and $S = 1$, (CuO-water)

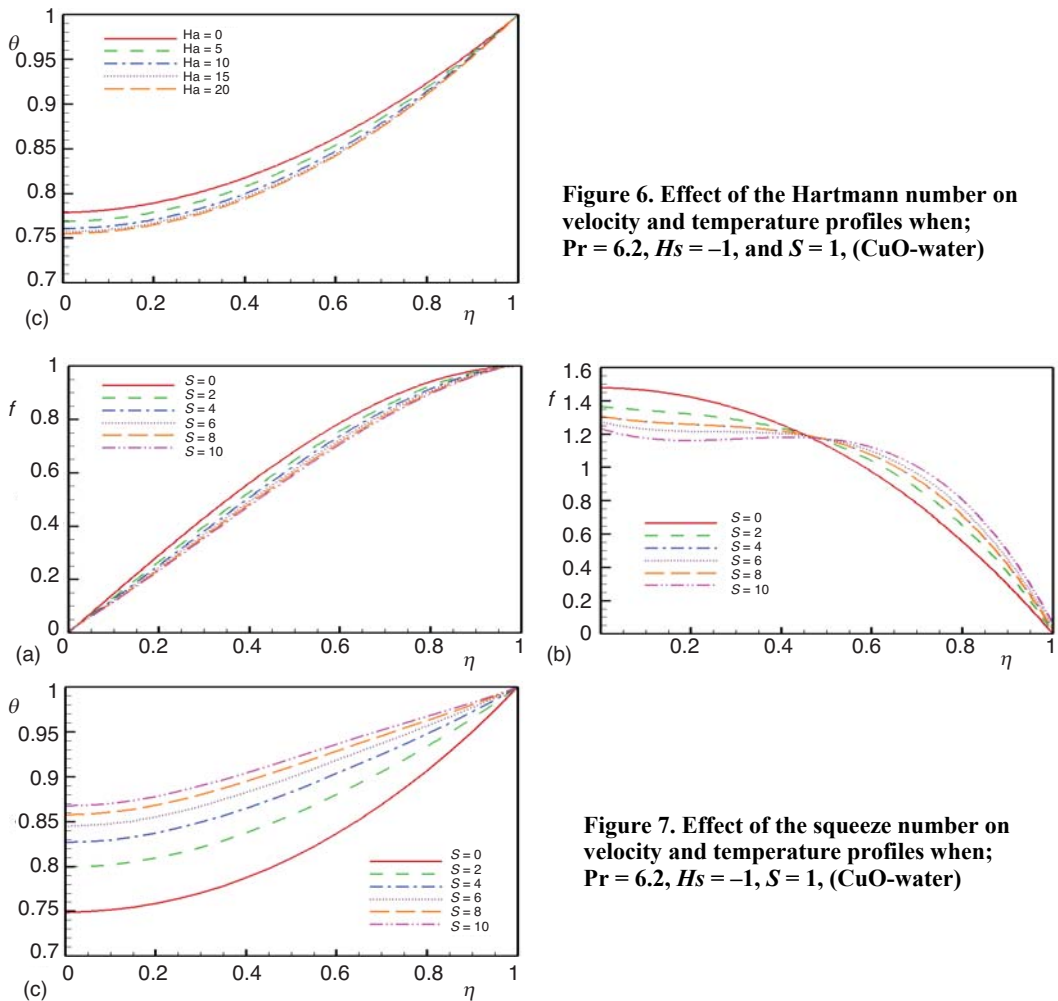


Figure 7. Effect of the squeeze number on velocity and temperature profiles when; $Pr = 6.2$, $Hs = -1$, $S = 1$, (CuO-water)

The effects of Hartmann number and squeeze number on Nusselt number and skin friction coefficient are displayed in fig. 8. As can be seen in this figure, Nusselt number has direct relationship with Hartman number and reverse with squeeze number. In order to, skin friction coefficient has direct relationship with both of Harman number and squeeze number. These effect are observed in contours of fig. 9. Figure 10 depicts the effects of heat source parameter on temperature profile, fig. 8(a), and Nusselt number, figs. 8(b) and 8(c). According to this figures, increasing in heat source parameter, temperature profile decreases, but Nusselt number increases that contour of fig. 8(c) confirm this effect.

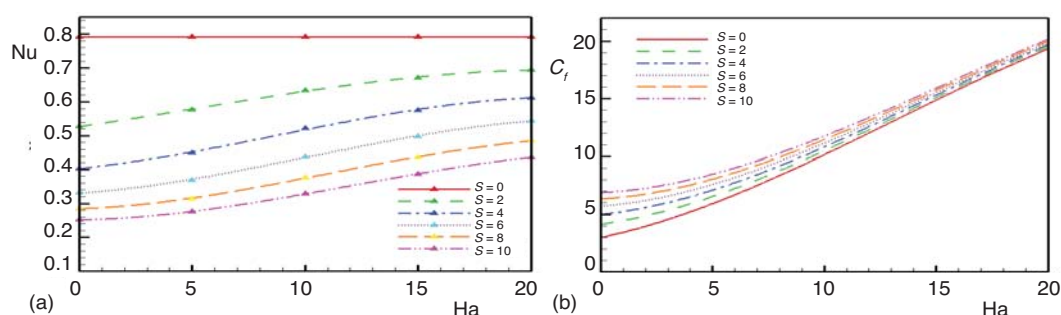


Figure 8. Effects of Hartmann number and squeeze number on (a) Nusselt number, (b) skin friction coefficient when; $\phi = 0.04$, $dp = 29$ nm, $Ha = 1$, $S = 1$, and $Hs = -1$ (CuO-water)

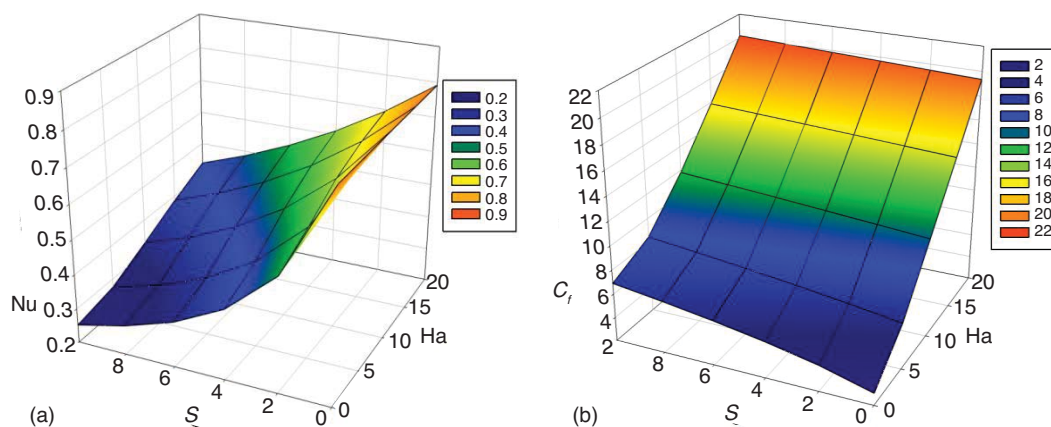


Figure 9. Contours for effects of squeeze number and Hartman number on (a) Nusselt number, (b) skin friction coefficient when; $\phi = 0.04$, $Hs = -1$, and $dp = 29$ nm (CuO-water)
(for color image see journal web site)

Conclusions

In this work, a thermal and flow analysis of an unsteady squeezing nanofluid flow and heat transfer using nanofluid based on Brinkman model in presence of variable magnetic field is investigated. The GM is applied to solve the non-linear differential equations governing the problem. As can be seen in results, the values of Nusselt number and skin friction coefficient for CuO-water is better than Al_2O_3 -water. Also-water, according to figures, as nanofluid volume fraction increases, Nusselt number increases and skin friction coefficient decreases, increase in the Hartman number results in an increase in velocity and temperature profiles and an increase in squeeze number can be associated with the decrease in the velocity.

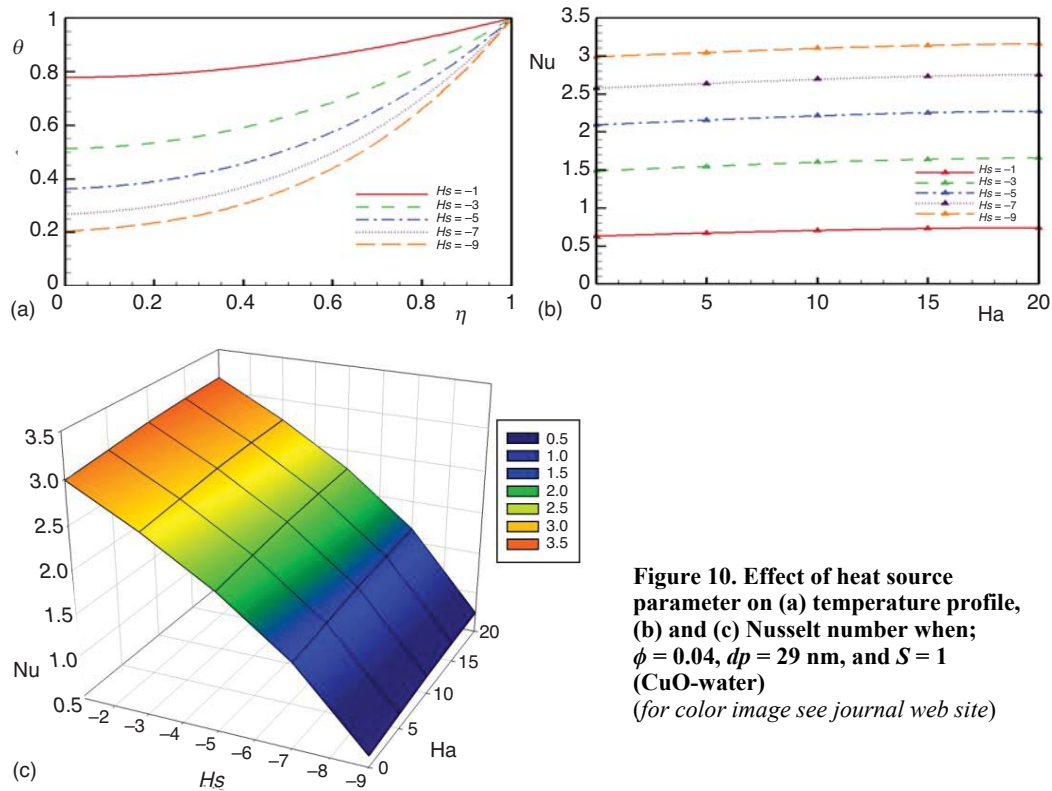


Figure 10. Effect of heat source parameter on (a) temperature profile, (b) and (c) Nusselt number when; $\phi = 0.04$, $dp = 29$ nm, and $S = 1$ (CuO-water) (for color image see journal web site)

Nomenclature

A_1, A_2, A_3, A_4 and A_5 – dimensionless constants, [–]
 C_p – specific heat capacity, [$\text{Jkg}^{-1}\text{K}^{-1}$]
 C_f – skin friction factor, [–]
 D – differential operator, [–]
 d_p – particle diameter, [mm]
 Ha – Hartman number, [–]
 H_s – heat source parameter, [–]
 k_{nf} – effective thermal conductivity of nanofluid, [$\text{Wm}^{-1}\text{K}^{-1}$]
 Nu – Nusselt number, [–]
 P – pressure, [Pa]
 Pr – Prandtl number, [–]
 S – squeeze number, [–]
 u – velocity in x- direction, [ms^{-1}]
 v – velocity in y- direction, [ms^{-1}]

Greek symbols

α – constant, [s^{-1}]
 ϕ – dimensionless concentration, [–]
 μ – dynamic viscosity, [Nsm^{-2}]
 ν – kinematic viscosity, [m^2s^{-1}]
 θ – dimensionless temperature, [–]
 ρ – fluid density, [kgm^{-3}]
 σ_{nf} – effective electrical conductivity of nanofluid

Subscripts

f – base fluid
 nf – nanofluid
 p – nanoparticle

References

- [1] Choi, S. U. S., Eastman, J. A., Enhancing Thermal Conductivity of Fluids with Nanoparticles, *ASME Fluids Eng. Div.*, 231 (1995), pp. 99-105
- [2] Das, S. K., et al., *Nanofluids: Science and Technology*, John Wiley and Sons, Hoboken, N. J., USA, 2007
- [3] Buongiorno, J., Convective Transport in Nanofluids, *ASME J. Heat Transf.*, 128 (2006), 3, pp. 240-250
- [4] Kakac, S., Pramuanjaroenkij, A., Review of Convective Heat Transfer Enhancement with Nanofluids, *International Journal of Heat and Mass Transfer*, 52 (2009), 13, pp. 3187-3196

- [5] Fan, J., Wang, L., Review of Heat Conduction in Nanofluids, *Journal of Heat Transfer*, 133 (2011), 4, 040801
- [6] Rahimi-Gorji, M., et al., Statistical Optimization of Microchannel Heat Sink (MCHS) Geometry Cooled by Different Nanofluids Using RSM Analysis, *The European Physical Journal Plus*, 130 (2015), 2, pp. 1-21
- [7] Malvandi, A., Ganji, D., Magnetic Field and Slip Effects on Free Convection inside a Vertical Enclosure Filled with Alumina/Water Nanofluid, *Chemical Engineering Research and Design*, 94 (2015), Feb., pp. 355-364
- [8] Mosayebidorcheh, S., et al., Approximate Solution of the Non-Linear Heat Transfer Equation of a Fin with the Power-Law Temperature-Dependent Thermal Conductivity and Heat Transfer Coefficient, *Propulsion and Power Research*, 3 (2014), 1, pp. 41-47
- [9] Joneidi, A., et al., Effect of Mass Transfer on a Flow in the Magnetohydrodynamic Squeeze Film between Two Parallel Disks with one Porous Disk, *Chemical Engineering Communications*, 198 (2010), 3, pp. 299-311
- [10] Pourmehran, O., et al., Heat Transfer and Flow Analysis of Nanofluid Flow Induced by a Stretching Sheet in the Presence of an External Magnetic Field, *Journal of the Taiwan Institute of Chemical Engineers*, 65 (2016), Aug., pp. 162-171
- [11] Khanafer, K., et al., Buoyancy-Driven Heat Transfer Enhancement in a Two-Dimensional Enclosure Utilizing Nanofluids, *International Journal of Heat and Mass Transfer*, 46 (2003), 19, pp. 3639-3653
- [12] Hatami, M., Ganji, D., Natural Convection of Sodium Alginate (SA) Non-Newtonian Nanofluid Flow between Two Vertical Flat Plates by Analytical and Numerical Methods, *Case Studies in Thermal Engineering*, 2 (2014), Mar., pp. 14-22
- [13] Pourmehran, O., et al., Numerical Optimization of Microchannel Heat Sink (MCHS) Performance Cooled by KKL Based Nanofluids in Saturated Porous Medium, *Journal of the Taiwan Institute of Chemical Engineers*, 55 (2015), Oct., pp. 49-68
- [14] Khan, W., Pop, I., Boundary-Layer Flow of a Nanofluid Past a Stretching Sheet, *International Journal of Heat and Mass Transfer*, 53 (2010), 11, pp. 2477-2483
- [15] Mahmood, M., et al., Squeezed Flow and Heat Transfer over a Porous Surface for Viscous Fluid, *Heat and Mass Transfer*, 44 (2007), 2, pp. 165-173
- [16] Domairry, G., Aziz, A., Approximate Analysis of MHD Squeeze Flow between Two Parallel Disks with Suction or Injection by Homotopy Perturbation Method, *Mathematical Problems in Engineering*, 2009 (2009), ID 603916
- [17] Ozisik, M. N., *Heat Conduction*, John Wiley & Sons, New York, USA, 1993
- [18] Rahimi-Gorji, M., et al., An Analytical Investigation on Unsteady Motion of Vertically Falling Spherical Particles in Non-Newtonian Fluid by Collocation Method, *Ain Shams Engineering Journal*, 6 (2014), 2, pp. 531-540
- [19] Pourmehran, O., et al., Analytical Investigation of Squeezing Unsteady Nanofluid Flow between Parallel Plates by LSM and CM, *Alexandria Engineering Journal*, 54 (2015), 1, pp. 17-26.
- [20] Hendi, F. A., Albugami, A. M., Numerical Solution for Fredholm-Volterra Integral Equation of the Second Kind by Using Collocation and Galerkin Methods, *Journal of King Saud University-Science*, 22 (2010), 1, pp. 37-40
- [21] Mohammadi, F., et al., Legendre Wavelet Galerkin Method for Solving Ordinary Differential Equations with Non-Analytic Solution, *International Journal of Systems Science*, 42 (2011), 4, pp. 579-585
- [22] Hatami, M., et al., Computer Simulation of MHD Blood Conveying Gold Nanoparticles as a Third Grade Non-Newtonian Nanofluid in a Hollow Porous Vessel, *Computer Methods and Programs in Biomedicine*, 113 (2014), 2, pp. 632-641
- [23] Brinkman, H., The Viscosity of Concentrated Suspensions and Solutions, *The Journal of Chemical Physics* 20 (1952), 4, p. 571
- [24] Oztop, H. F., Abu-Nada, E., Numerical Study of Natural Convection in Partially Heated Rectangular Enclosures Filled with Nanofluids, *International Journal of Heat and Fluid Flow*, 29 (2008), 5, pp. 1326-1336
- [25] Mustafa, M., et al., On Heat and Mass Transfer in the Unsteady Squeezing Flow between Parallel Plates, *Meccanica*, 47 (2012), 7, pp. 1581-1589